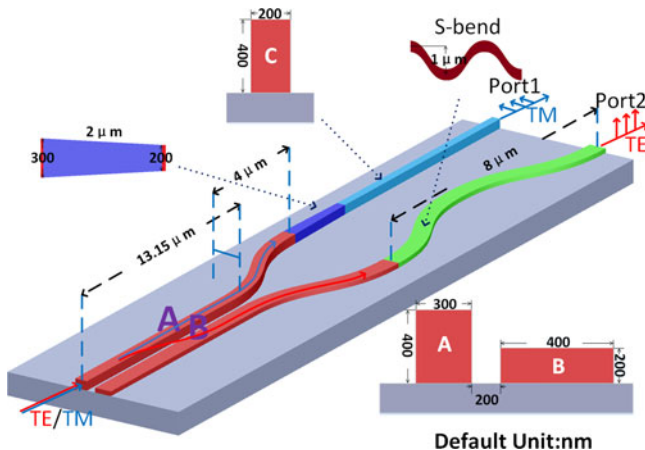


Ultrahigh Suppression Broadband Polarization Splitter Based on an Asymmetrical Directional Coupler

Volume 9, Number 5, October 2017

Can Liu
Lianshan Yan, *Senior Member, IEEE*
Anlin Yi
Hengyun Jiang
Yan Pan
Lin Jiang
Xia Feng
Wei Pan
Bin Luo



DOI: 10.1109/JPHOT.2017.2750218
1943-0655 © 2017 IEEE

Ultrahigh Suppression Broadband Polarization Splitter Based on an Asymmetrical Directional Coupler

Can Liu, Lianshan Yan, *Senior Member, IEEE*, Anlin Yi,
Hengyun Jiang, Yan Pan, Lin Jiang, Xia Feng, Wei Pan, and Bin Luo

Center for Information Photonics and Communications, School of Information Science and Technology, Southwest Jiaotong University, Chengdu 610031, China

DOI:10.1109/JPHOT.2017.2750218

1943-0655 © 2017 IEEE. Translations and content mining are permitted for academic research only.
Personal use is also permitted, but republication/redistribution requires IEEE permission.
See http://www.ieee.org/publications_standards/publications/rights/index.html for more information.

Manuscript received July 29, 2017; revised August 30, 2017; accepted September 5, 2017. Date of publication September 8, 2017; date of current version September 21, 2017. The work was supported in part by the National Basic Research Program of China under Grant 2013CBA01700, in part by the Natural Science Foundation of China under Grants 61335005 and 61325023, and in part by the Research Fund for the Doctoral Program of Higher Education of China under Grant 20130184110015. Corresponding author: L. Yan (e-mail: lsyan@home.swjtu.edu.cn).

Abstract: Polarization-beam-splitters with both broadband operation window and high extinction ratio are highly desirable in optical communication systems. In this paper, a compact noncascaded-directional-couplers PBS with an ultrahigh extinction ratio and low excess loss is proposed. The PBS utilizes an asymmetrical directional coupling structure consisted of a TE-pass-polarizer waveguide and a TE- and TM-pass waveguide. The simulation results show that the extinction ratio is up to 35.41 dB and the excess loss is only 0.11 dB around the central wavelength 1550 nm for both polarizations (TE and TM). Meanwhile, when the extinction ratio is 30, 25, and 20 dB, the corresponding bandwidth is 72, 145, and 188 nm, respectively. Also, the EL is 1 and 0.5 dB in a bandwidth of ~73 and ~48 nm, respectively. A fabrication tolerance of ±10 nm for the waveguide width is also achieved.

Index Terms: Guided waves, integrated optics devices, polarization-selective devices, silicon-on-insulator.

1. Introduction

Polarization beam splitters (PBSs) are basic elements for polarization manipulation in state-of-the-art polarization-multiplexed systems [1]. In particular, compact or high extinction ratio(ER) PBSs based on photonic-integrated circuits (PICs) are widely achieved. More importantly, key features, such as broad bandwidth, low excess loss (EL) and high ER, are highly desirable for high-speed polarization-division-multiplexed (PDM) systems [2]. So far several kinds of integrated PBSs based on different configurations have been demonstrated, including multimode interference (MMI) [3], [4], Mach-Zehnder interferometers (MZIs) [5], directional couplers (DCs) [6]–[8], photonic-crystals (PhCs) [9], and gratings [10]–[13]. Although directional couplers (DCs) [8] provide a good approach to broaden the working bandwidth, they have relatively complex structure. In spite of Adiabatic coupler [15] has low EL, it's ER not high yet. Most PBSs based on directional coupler have advantages of compact size and broadband compared to those based on MMI and MZIs or grating-assisted couplers. The PBSs utilizing grating-assisted couplers [16] can get a high ER but have a narrow bandwidth. Among these structures, asymmetric DCs [7] have been regarded as one of the most

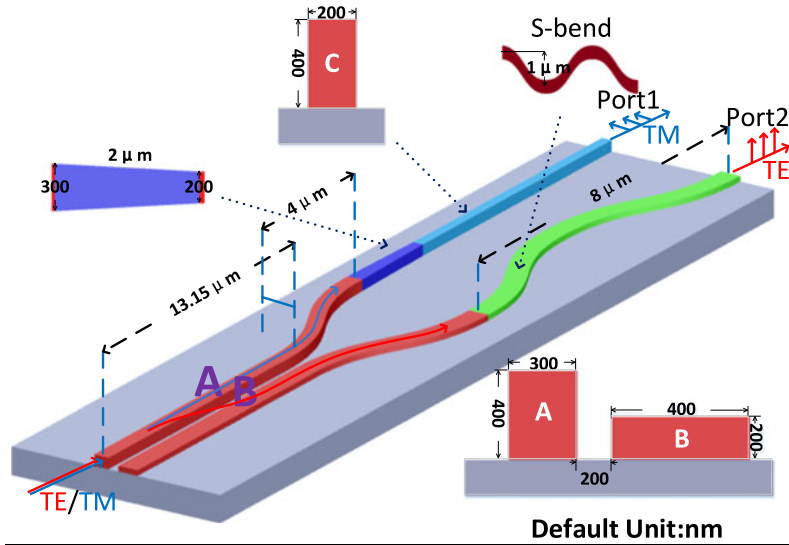


Fig. 1. The structure of proposed PBS: waveguide A: $300 \text{ nm} \times 400 \text{ nm}$ (wide \times thickness); waveguide B: $400 \text{ nm} \times 200 \text{ nm}$; waveguide C: $200 \text{ nm} \times 400 \text{ nm}$; gap: 200 nm .

attractive options, because of the performance excellence and design simplicity, however the ER of TE polarization is not very high yet by reason of some undesired residual cross-coupling in the DC [7]. In addition, the design in [14] based on improved structure consisted of three cascaded DCs [7] coupling system, thus the ER is naturally higher than a one-stage coupling system [7]. Therefore, it is very critical to develop compact high-performance PBSs with a low EL and a high ER in a broad bandwidth.

In this paper, we propose a novel compact non-cascaded-directional-couplers PBS with an ultrahigh ER and low EL on silicon-on-insulator (SOI) platform. The PBS utilizes the asymmetrical directional coupling structure consisted of two strip-nanowire waveguides with different sizes. The waveguide A of proposed PBS can contain both (TE and TM) polarizations beam, while the waveguides B/C of proposed PBS only contain single (TE/TM) polarization beam. Using commercial 3D-FDTD simulation software (i.e., the Lumerical Solutions, Inc.), the results show that the ER is up to 35.41 dB and the EL is only 0.11 dB around the central wavelength 1550 nm for both polarizations (TE and TM). Meanwhile, when the ER is 30 , 25 and 20 dB , the corresponding bandwidth is 72 , 145 and 188 nm , respectively. Also, the EL is 1 and 0.5 dB in a bandwidth of ~ 73 and $\sim 48 \text{ nm}$, respectively. A fabrication tolerance of $\pm 10 \text{ nm}$ for the waveguide width is also achieved.

2. Theory and Device Design

The structure of the proposed PBS is shown in Fig. 1, which includes an asymmetrical directional coupler consisted of two strip-nanowire silicon waveguides with different thicknesses and widths.

The directional coupler is composed of two parallel silicon waveguides. The cladding is air and the substrate of the PBS is silica with a thickness of $2 \mu\text{m}$. The refractive indices of Si (n_{Si}), SiO_2 (n_{Silica}) and air (n_{Air}) are 3.477 , 1.44 and 1.0 , respectively.

As shown in Fig. 1, the cross-section (wide \times thickness) of this waveguide specially is set as $300 \times 400 \text{ nm}$. The corresponding effective indexes of TE and TM mode are calculated to be 2.020 and 2.397 at 1550 nm (see Table 1). Then, waveguide A can contain fundamental TE and TM modes due to that the effective index is more than 1.45 . In order to realize the PBS function, the input TE beams in waveguide A have to be coupled into waveguide B by an asymmetrical directional couplers (as shown in Fig. 1), but the input TM beams must propagate through the waveguide A.

TABLE 1
The Effective Index of Waveguide A, B, and C at 1550 nm

Waveguide	Cross Section [nm]	Effective Index TE	Effective Index TM
A	300 × 400	2.020	2.397
B	400 × 200	2.020	NA
C	200 × 400	NA	2.018

NA: Not available.

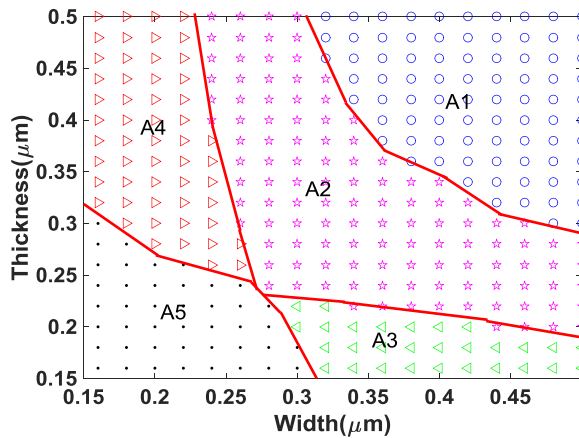


Fig. 2. Modal characteristics of silicon waveguide with different width and thickness at 1550 nm.

Therefore, the coupled waveguides (A and B) have to satisfy the phase-matching condition for the evanescent coupling. That is to say, the effective index of waveguide A TE-mode is equal to the effective index of waveguide B TE-mode (see Table 1).

The eigenmodes of the waveguide with a width and thickness from $0.16\text{ }\mu\text{m}$ to $0.5\text{ }\mu\text{m}$ are calculated. The modal characteristics of the waveguide are shown in Fig. 2, which consists of five regions labeled from A1 to A5 with different marks. Region A1: multimode region; Region A2: single-mode region; Region A3: single-TE-mode region; Region A4: single-TM-mode region; and Region A5: cutoff region. It can be observed that waveguide with a cross section in region A3 only supports TE mode, while for region A4, it only supports TM mode. Therefore the waveguide A contains single-mode, the waveguide B only contains single-TE-mode and the waveguide C only contains single-TM-mode.

To make waveguides B and C work as TE and TM-pass-polarizer, the width of waveguide C is set as 200 nm and the thickness of waveguide B is set as 200 nm (also [16] and [17]). The final sizes of waveguides B and C are set as $400 \times 200\text{ nm}$ and $200 \times 400\text{ nm}$, respectively. Subsequently waveguides A and C are TM- and TE-pass polarizer, respectively. In addition, the waveguide A is connected with the waveguide C by the taper waveguide which brings a small loss for the TM beams.

Next, the coupling coefficient of directional couplers must be properly chosen by setting the coupling length and the gap between two waveguides. Here, the gap is specially set as 200 nm (the normal gap in commercial fabrication procedures) to enhance the contra-directional coupling strength. And the bending radius (R) of waveguide A, B are set as $3.33\text{ }\mu\text{m}$ to ensure that the bending loss is negligible for fundamental modes.

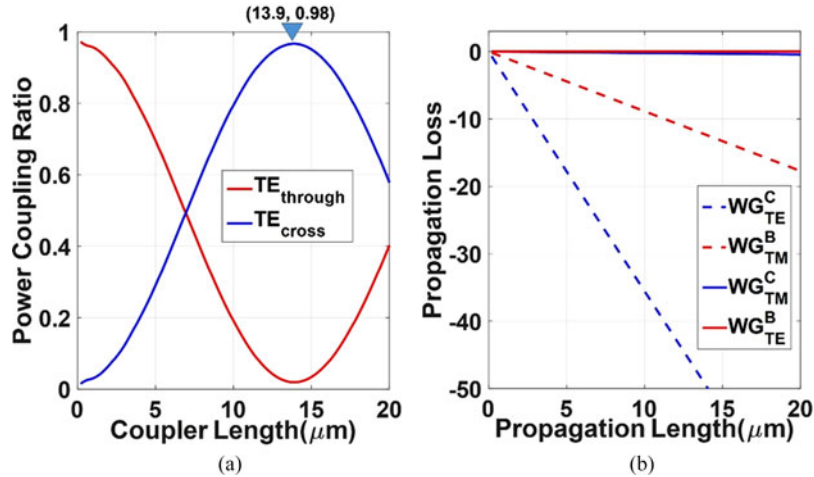


Fig. 3. (a) The power coupling ratio of directional couplers related to the coupling length for TE mode at 1550 nm. (b) Performance of the polarizer (TE and TM) at 1550 nm. WG: waveguide.

The behavior of an asymmetrical directional coupler can be formulated by coupled mode theory [18]. The fraction of the power (P_{cross}), which is coupled from one waveguide to the other, can be expressed as:

$$P_{\text{cross}} = P_{\text{in}} \times \frac{k^2}{g^2} \sin^2(gz) e^{-\alpha z} \quad (1)$$

$$g^2 = k^2 + \left(\frac{\Delta\beta}{2} \right)^2 \quad (2)$$

where $\Delta\beta$ is a phase constant difference, P_{in} is the input optical power of the waveguide, z is the total effective coupling length of DC that includes the two parts (i.e., straight and bent waveguides). The optical loss coefficient of α in both waveguides is an exponential function. The coupling coefficient k is a strong function of the shape of the mode tails in the guides. The performance of an asymmetrical directional coupler is shown in Fig. 3(a) at the condition of the input wavelength is 1550 nm. It can be observed that the coupling power achieves 98% for the TE polarization when the total coupler length (Z_{TE}) is 13.9 μm . The bend part of waveguide A and C, as well as the separating ports, can also couple some power which is assumed as $k_{0-\text{TE}}$. According to (1) and (2), the bend part can be converted into the equivalent straight length ($Z_{0-\text{TE}}$). Thus the straight part of coupler length $Z_{1-\text{TE}}$ can be calculated by $Z_{1-\text{TE}} = Z_{\text{TE}} - Z_{0-\text{TE}}$. For the best effective coupling, the length of the straight part is 13.15 μm . At last, the total length of the PBS is 25.15 μm (as shown in Fig. 1).

Owing to the wavelength-dependent power coupling, it's not easy to split the polarization beam at high ER for a relative broad band. In the proposed PBS, waveguides B and C are specially designed to merely hold single polarization, which can further filter out those unwanted polarization components from the power coupling. That is to say, waveguide B is a TE-pass polarizer due to that the waveguide B cannot sustain TM mode, and waveguide C is a TM-pass polarizer due to that the waveguide C cannot sustain TE mode.

The performance of TE-pass polarizer and TM-pass polarizer at difference polarization (TE/TM) for waveguides B and C is shown in the Fig. 3(b). It can be observed that when TE/TM polarization beam propagates in the waveguide C/B, it will suffer from a huge loss. That is to say, the waveguide B/C only sustains fundamental TE/TM mode. As shown in Fig. 4(a) and (b), it determines the mode condition for the waveguide that the width of the waveguide is varied from 100 nm to 1000 nm at different thickness 400 nm [see Fig. 4(a)] and 200 nm [see Fig. 4(b)]. Obviously, waveguide B

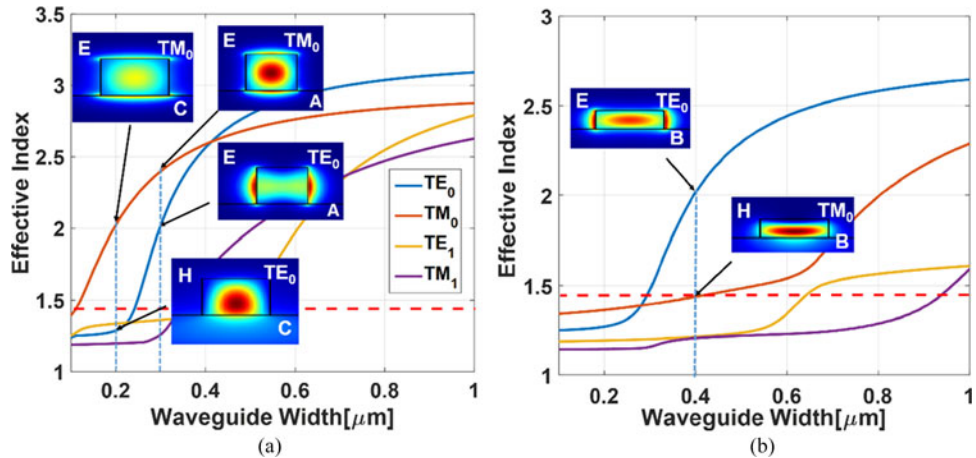


Fig. 4. Simulation of the effective index of the waveguide modes versus the width of a strip waveguide at 1550 nm (a) Waveguide thickness 400 nm (b) Waveguide thickness 200 nm E: E-field intensity; H: H-field intensity A/B/C: Waveguide A/B/C::

and C only support single TE or TM polarization mode. Meanwhile, waveguide A can support both polarizations (TM and TE) because it can well confine the energy of both polarizations. In addition, all waveguides (A, B and C) cannot support higher-order modes because of the corresponding effective indexes are less than 1.45, which mean that the beam propagates in the waveguide, it will suffer from a huge loss.

3. Simulation Results and Discussion

The power field profiles of the light propagation in the designed PBS are shown in Fig. 5 for TE [see Fig. 5(a)] and TM [see Fig. 5(b)] polarizations at 1550 nm wavelength. It is shown that TE polarization is coupled and output from the cross port, meanwhile, TM polarization is output from the through port without any coupling. Considering the bending loss is polarization dependent, i.e., TM fundamental mode has a higher bending loss than TE fundamental mode for the waveguide B. Therefore, a sharp S-bending structure can enhance TE-pass polarizer function which helps filter out the undesired TM polarization at this port and improves the ER. Furthermore, the bending loss in waveguide B is negligible for TE polarization, and the end separation ($1 \sim 2 \mu\text{m}$) of the two output ports is large enough to avoid any undesired coupling. Note that, even though the power profiles distribute different for the difference size of waveguides, the total output intensity of two branches are almost the same.

The calculated transmission spectral responses are shown in Fig. 6 at different ports for TE and TM polarizations. It is shown that the ER is 35.41 dB and the EL is 0.11 dB around the central wavelength 1550 nm for both polarizations. At the same time, the wavelength range from 1.517 to 1.586 μm , the PBS's corresponding suppression ratio is 30 dB and the operation bandwidth is 69 nm with an EL is <1 db. Meanwhile, the EL is 1 dB and 0.5 dB in a bandwidth of ~ 74 nm and ~ 48 nm, respectively. Moreover, Fig. 6(b) shows the ER of the PBS for both TE and TM polarizations. When the ER is 30 dB, 25 dB and 20 dB, the corresponding bandwidth is 72 nm, 145 nm and 188 nm, respectively.

The fabrication tolerance is very important for fabricating a chip. By assuming that there is a core-width variation Δw or core-thickness variation Δh , the waveguide width has $W_{\text{WG}} = W_{\text{WG}} + \Delta w$. Correspondingly, the gap widths are given as $W_{\text{gap}} = W_{\text{gap}} - \Delta w$ or the waveguide thickness has $H_{\text{WG}} = H_{\text{WG}} + \Delta h$. In this way, it becomes tolerant to the etching depth. Therefore, we give an analysis for the case in which there is a waveguide width variation $\Delta w = \pm 5 \text{ nm}$ and $\pm 10 \text{ nm}$ or waveguide thickness variation $\Delta h = \pm 5 \text{ nm}$ (as shown in Fig. 7). It can be seen that the central

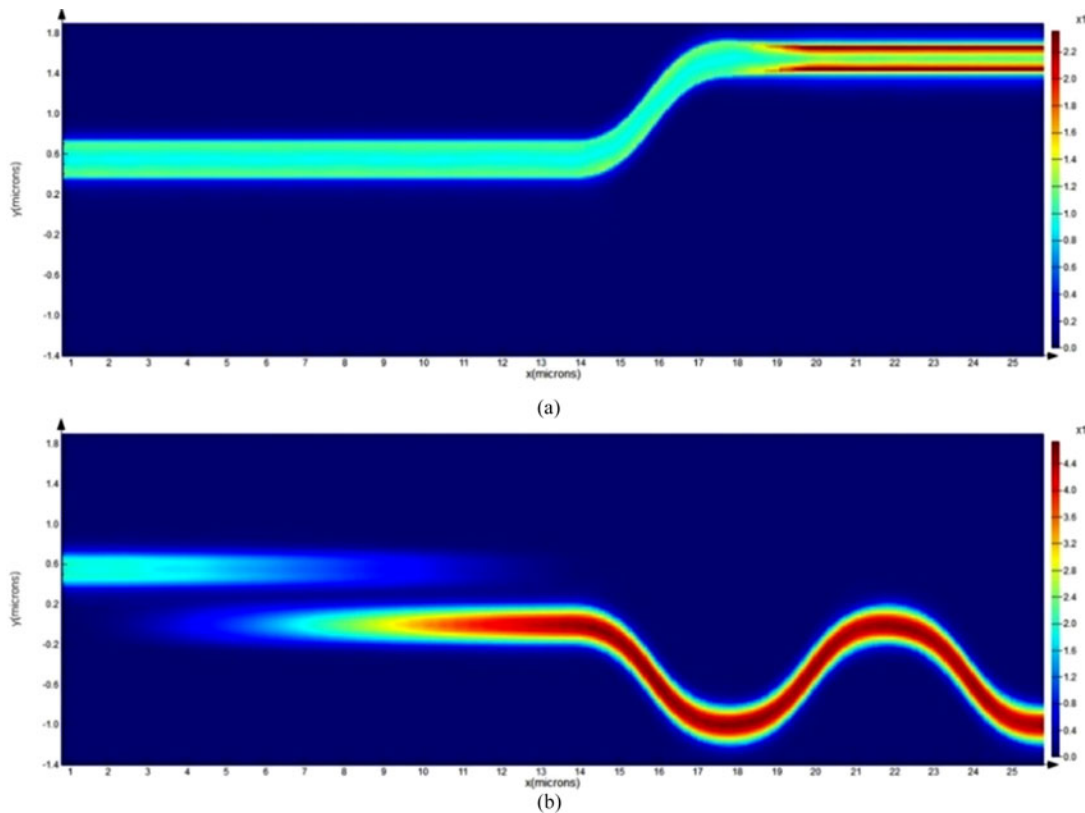


Fig. 5. The power field profile of designed PBS at 1550 nm: (a) TM and (b) TE.

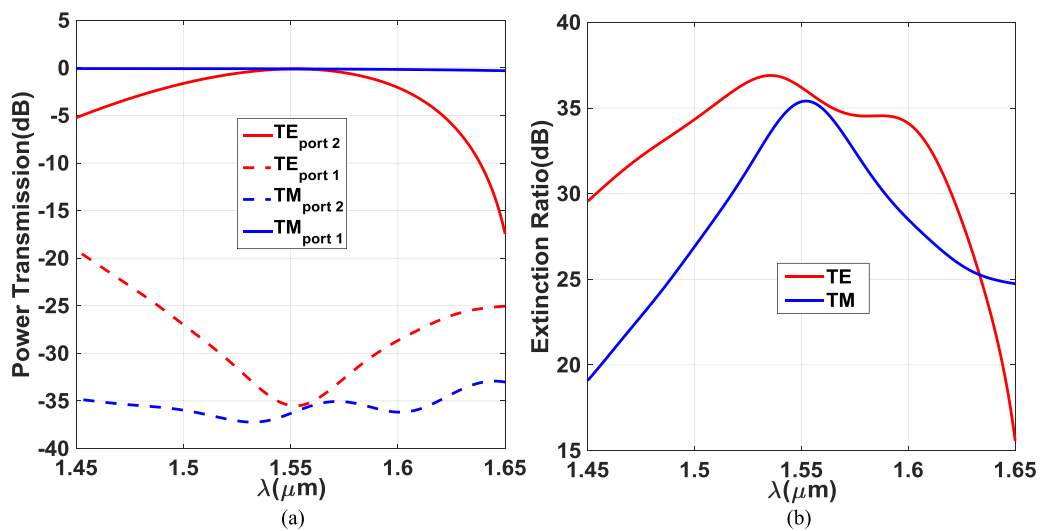


Fig. 6. (a) Transmission spectral responses of the PBS (b) Extinction ratio of the PBS.

wavelength moved slightly, the ER is reduced and the EL is increased. However the PBS still has a >20 dB ER over a very broad wavelength band (>100 nm) for both polarizations, even when the width variation $\Delta w = \pm 10$ nm or the thickness variation $\Delta h = \pm 5$ nm. Hence, a fabrication tolerance of ± 10 nm for the waveguide width is also achieved.

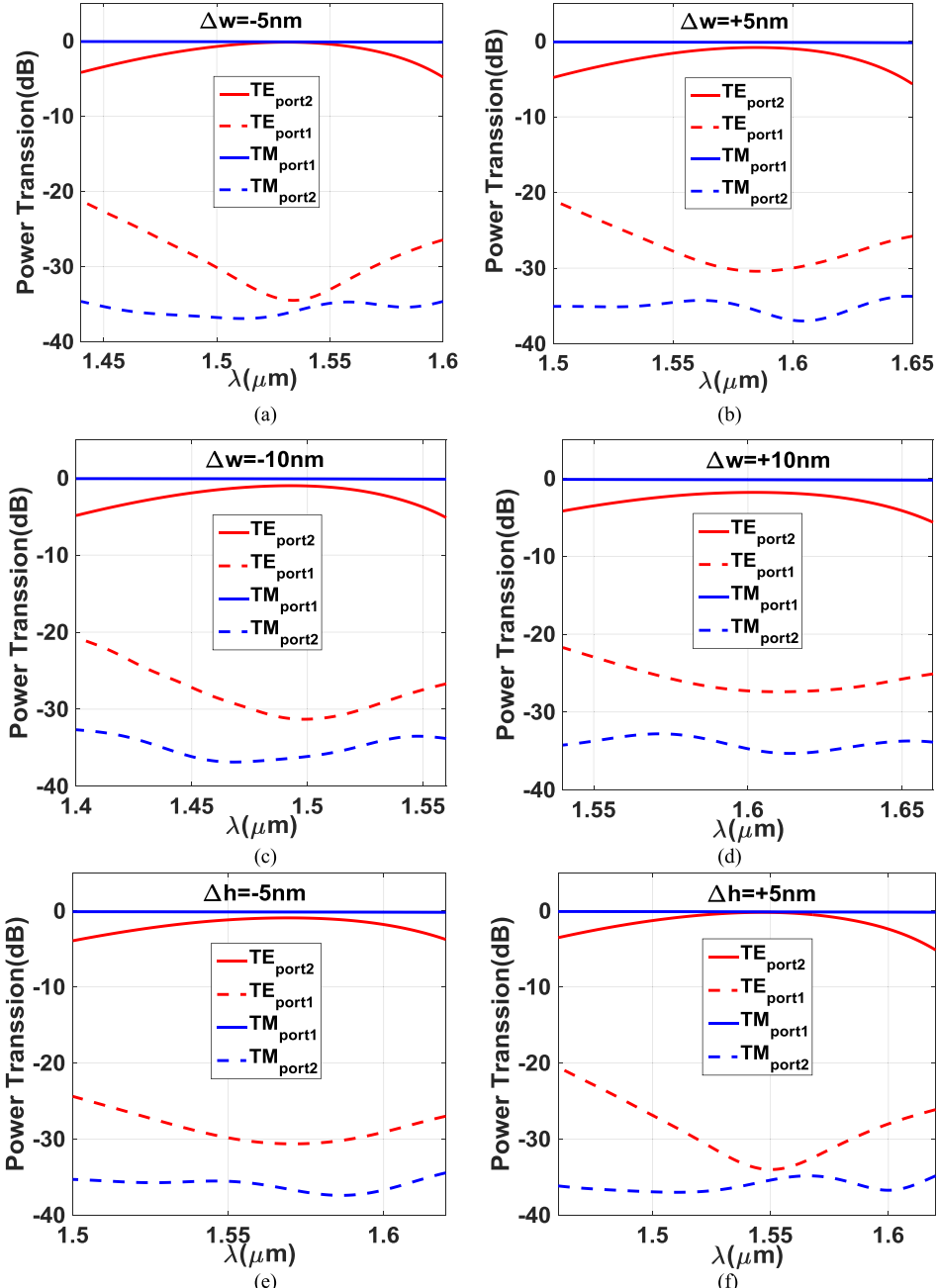


Fig. 7. Transmission spectral responses of the PBS when there is a core-width variation Δw or core-thickness variation Δh . (a) $\Delta w = -5 \text{ nm}$; (b) $\Delta w = +5 \text{ nm}$; (c) $\Delta w = -10 \text{ nm}$; (d) $\Delta w = +10 \text{ nm}$; (e) $\Delta h = -5 \text{ nm}$; (f) $\Delta h = +5 \text{ nm}$.

We further compare our work with those high-performance PBSs, they have been reported so far in PICs as listed in Table 2. It is shown that the present PBS is not only the best one with ultra-broad bandwidth for achieving a high ER (e.g., $> 30 \text{ dB}$) and a low EL (e.g., $< 0.5 \text{ dB}$), but also non-cascaded-DCs structure. In terms of the manufacture feasibility, [1] shows a way to fabricate two kinds of waveguide thicknesses. With the development of the silicon photonics fabrication, it will quite possible to fabricate multiple-thickness waveguides in one chip in the near future.

TABLE 2
High-Performance Comparison of State-of-the-Art PBSs in PICs

Structure	ER	EL	BW _{20dB} ER	BW _{25dB} ER	BW _{30dB} ER	Length [μm]	Cascaded
Symmetric DC[8]	25 dB	0.5 dB	125 nm	NA	NA	97.4	Yes
Grating [13]	30 dB	1 dB	29 nm	25 nm	21 nm	27.5	No
Bend DC[14]	35 dB	0.35 dB	135 nm	95 nm	70 nm	20	Yes
This work	35.41 dB	0.11 dB	188 nm	145 nm	72 nm	25.15	No

NA: Not available. BW_{20dB}ER, BW_{25dB}ER and BW_{30dB}ER are the bandwidths for a >20 dB, >25 dB and >30 dB ER.

4. Conclusion

We propose a novel compact non-cascaded-DCs PBS with ultra-high ER and low EL. The PBS utilizes an asymmetrical DC structure consisted of a TE- and TM-pass waveguide and TE-pass-polarizer waveguides. An integrated compact footprint (i.e., $2.3 \times 25.15 \mu\text{m}^2$) PBS has been demonstrated. The simulated results show that the ER is 35.41 dB and the EL is 0.11 dB around the central wavelength 1550 nm for both polarizations (TE and TM). Meanwhile, when the ER is 30, 25 and 20 dB, the corresponding bandwidth is 72, 145 and 188 nm, respectively. Also, the EL is 1 and 0.5 dB in a bandwidth of ~ 73 and ~ 48 nm, respectively. A fabrication tolerance of ± 10 nm for the waveguides width is also obtained. The proposed PBS may be a desired candidate for prominent Tbit/s polarization-division-multiplexed (PDM) systems.

References

- [1] T. Barwicz *et al.*, "Polarization-transparent microphotonic devices in the strong confinement limit," *Nature Photon.*, vol. 1, pp. 57–60, 2007.
- [2] D. Dai, J. Bauters, and J. E. Bowers, "Passive technologies for future large-scale photonic integrated circuits on silicon: Polarization handling, light non-reciprocity and loss reduction," *Light Sci. Appl.*, vol. 1, 2012, Art. no. e1.
- [3] B.-K. Yang, S.-Y. Shin, and D. Zhang, "Ultrashort polarization splitter using two-mode interference in silicon photonic wires," *IEEE Photon. Technol. Lett.*, vol. 21, no. 7, pp. 432–434, Apr. 2009.
- [4] M. Yin, W. Yang, Y. Li, X. Wang, and H. Li, "CMOS-compatible and fabrication-tolerant MMI-based polarization beam splitter," *Opt. Commun.*, vol. 335, pp. 48–52, 2015.
- [5] L. M. Augustin, R. Hanfouq, J. J. G. M. van der Tol, W. J. M. de Laat, and M. K. Smit, "A compact integrated polarization splitter/converter in InGaAsP-InP," *IEEE Photon. Technol. Lett.*, vol. 19, no. 17, pp. 1286–1288, Sep. 2007.
- [6] D. Dai, Z. Wang, and J. E. Bowers, "Ultrashort broadband polarization beam splitter based on an asymmetrical directional coupler," *Opt. Lett.*, vol. 36, no. 13, pp. 2590–2592, 2011.
- [7] D. Dai and J. E. Bowers, "Novel ultra-short and ultra-broadband polarization beam splitter based on a bent directional coupler," *Opt. Exp.*, vol. 19, no. 19, pp. 18614–18620, 2011.
- [8] Z. Lu, Y. Wang, F. Zhang, N. A. F. Jaeger, and L. Chrostowski, "Wideband silicon photonic polarization beamsplitter based on point-symmetric cascaded broadband couplers," *Opt. Exp.*, vol. 23, no. 23, pp. 29413–29422, 2015.
- [9] N. Saidani, W. Belhadj, F. AbdelMalek, and H. Bouchriha, "Detailed investigation of self-imaging in multimode photonic crystal waveguides for applications in power and polarization beam splitters," *Opt. Commun.*, vol. 285, no. 16, pp. 3487–3492, 2012.
- [10] J. Feng and Z. Zhou, "Polarization beam splitter using a binary blazed grating coupler," *Opt. Lett.*, vol. 32, no. 12, pp. 1662–1664, 2007.
- [11] X. Guan, P. Chen, S. Chen, P. Xu, Y. Shi, and D. Dai, "Low-loss ultracompact transverse-magnetic-pass polarizer with a silicon subwavelength grating waveguide," *Opt. Lett.*, vol. 39, no. 15, pp. 4514–4517, 2014.
- [12] H. Qiu, Y. Su, P. Yu, T. Hu, J. Yang, and X. Jiang, "Compact polarization splitter based on silicon grating-assisted couplers," *Opt. Lett.*, vol. 40, no. 9, pp. 1885–1887, 2015.
- [13] Y. Zhang *et al.*, "High-extinction-ratio silicon polarization beam splitter with tolerance to waveguide width and coupling length variations," *Opt. Exp.*, vol. 24, no. 6, pp. 6586–6593, 2016.
- [14] H. Wu, Y. Tan, and D. Dai, "Ultra-broadband high-performance polarizing beam splitter on silicon," *Opt. Exp.*, vol. 25, no. 6, pp. 6069–6075, 2017.

- [15] H. Cai *et al.*, "An adiabatic/ diabatic polarization beam splitter," in *Proc. Int. Conf. IEEE Opt. Interconnects*, pp. 102–103, 2016.
- [16] S. I. H. Azzam, M. F. O. Hameed, N. F. F. Areed, M. M. Abd-Elrazzak, H. A. El-Mikaty, and S. S. A. Obayya, "Proposal of an ultracompact CMOS-compatible TE/TM-pass polarizer based on Sol platform," *IEEE Photon. Technol. Lett.*, vol. 26, no. 16, pp. 1633–1636, Aug. 2014.
- [17] Q. Wang and S. T. Ho, "Ultracompact TM-pass silicon nanophotonic waveguide polarizer and design," *IEEE Photon. J.*, vol. 2, no. 1, pp. 49–56, Feb. 2010.
- [18] R. G. Hunsperger, "Integrated optics: Theory and technology," *Appl. Opt.*, vol. 31, no. 3, pp. 391–409, 1992.
- [19] J. T. Kim and S. Park, "Vertical polarization beam splitter using a hybrid long-range surface plasmon polariton waveguide," *J. Opt.*, vol. 16, no. 2, 2014, Art. no. 025501.